

TRACING PERIODIC ORBITS IN 3D GALACTIC POTENTIALS BY THE PARTICLE SWARM OPTIMIZATION METHOD

Charalampos D. Skokos^{*†}, Konstantinos E. Parsopoulos^{‡§}, Panos A. Patsis^{*}, and Michael N. Vrahatis^{‡§}

^{*} Research Center for Astronomy and Applied Mathematics, Academy of Athens
14 Anagnostopoulou str., GR-10673 Athens, Greece
e-mail: hskokos@cc.uoa.gr, web page: <http://www.math.upatras.gr/~skokos>

[†] Center for Research and Applications of Nonlinear Systems
University of Patras, GR-26500 Patras, Greece

[‡] Department of Mathematics, University of Patras
GR-26110 Patras, Greece

[§] University of Patras Artificial Intelligence Research Center (UPAIRC), University of Patras
GR-26110 Patras, Greece

Keywords: Particle Swarm Optimization, Barred galaxies, Periodic orbits.

Abstract. *The class of Swarm Intelligence algorithms consists of stochastic optimization methods that exploit a population of interacting individuals to probe the search space simultaneously. The ability to work on non-differentiable and discontinuous functions using only function value information renders these algorithms a useful tool, especially in cases where classical optimization methods fail. In this contribution, we apply Particle Swarm Optimization for locating periodic orbits in a 3D Ferrers bar model. An appropriate scheme that transforms the problem of finding periodic orbits to the corresponding problem of detecting the global minimizers of a function defined on the Poincaré Surface of Section of the Hamiltonian system is employed. We succeeded in tracing systematically several periodic orbits of the system, a large fraction of which is reported for the first time. In particular, we found families of 2D and 3D periodic orbits, associated with inner resonance higher than the 8:1 resonance, and not belonging to the x1-tree. We were also able to locate a plethora of p-periodic orbits with $p > 1$.*

1 DESCRIPTION OF THE ALGORITHM

1.1 The Particle Swarm Optimization algorithm

Particle Swarm Optimization (PSO) belongs to the category of Swarm Intelligence methods. The ideas that underlie PSO are inspired by the social dynamics of flocking organisms, which are governed by fundamental rules like nearest-neighbor velocity matching and information sharing.

Assume the problem of finding a global minimizer of an n-dimensional function, f , which is called the *objective function*, defined in an n-dimensional search space, $S \subset \mathbf{R}^n$. PSO is a population based algorithm, i.e., it exploits a population of individuals to probe promising regions of the search space, simultaneously. In this context, the population is called a *swarm* and the individuals (i.e., the search points) are called *particles*. Each particle moves with an adaptable velocity within the search space, and retains a memory of the best position it ever encountered. In minimization problems, the best positions are characterized by lower function values. In the local variant of PSO, each particle is assigned to a neighborhood that consists of a pre-specified number of particles, and the best position ever attained by the particles that comprise the neighborhood is communicated among them. On the other hand, in the global variant of PSO, the whole swarm is considered as the neighborhood of each particle. The local variant is characterized by better exploration behavior, i.e., more thorough search, while the global variant has better exploitation capabilities, i.e., faster convergence towards the best solutions detected so far. In the current work, we employed the local variant, due to its better exploration capabilities in multimodal problems, such as the detection of periodic orbits.

Consider a swarm consisting of N particles. Each particle is an n-dimensional vector in S ,

$$\mathbf{X}_i = (x_{i1}, x_{i2}, \dots, x_{in})^T \in S, \quad i=1,2,\dots,N, \quad (1)$$

where $(^T)$ denotes the transpose of a matrix. The velocities of the particles are also n-dimensional vectors,

$$\mathbf{V}_i = (u_{i1}, u_{i2}, \dots, u_{in})^T, \quad i=1,2,\dots,N. \quad (2)$$

The best previous position encountered by the i-th particle is a point in S, denoted by

$$\mathbf{P}_i = (p_{i1}, p_{i2}, \dots, p_{in})^T \in S. \quad (3)$$

The positions, X_i , as well as the velocities, V_i , are initialized randomly and uniformly within S. The best positions, P_i , are initially set equal to X_i . Each particle is evaluated according to the objective function, f , i.e., the value $f(X_i)$ is computed for all particles. Obviously, at the initialization phase, it holds that $f(P_i) = f(X_i)$.

Let $N_i = (X_{i-r}, \dots, X_{i-1}, X_i, X_{i+1}, \dots, X_{i+r})$, be a neighborhood of radius r of the i-th particle, X_i . Then g_i is defined as the index of the best particle in the neighborhood of X_i , i.e.,

$$f(\mathbf{P}_{g_i}) \leq f(\mathbf{P}_j), \quad j=i-r, \dots, i+r. \quad (4)$$

The neighborhood's topology is usually cyclic, i.e., the first particle, X_1 , is assumed to follow after the last particle, X_N . For example, a neighborhood of radius 3 of the particle X_2 consists of the particles X_{N-1} , X_N , X_1 , X_2 , X_3 , X_4 and X_5 .

The particles are moving in S according to the equations^[1]:

$$\mathbf{V}_i^{(q+1)} = \chi \left(\mathbf{V}_i^{(q)} + c_1 r_1 (\mathbf{P}_i^{(q)} - \mathbf{X}_i^{(q)}) + c_2 r_2 (\mathbf{P}_{g_i}^{(q)} - \mathbf{X}_i^{(q)}) \right), \quad (5)$$

$$\mathbf{X}_i^{(q+1)} = \mathbf{X}_i^{(q)} + \mathbf{V}_i^{(q+1)}, \quad (6)$$

where $i = 1, 2, \dots, N$; χ is a parameter called *constriction factor*; c_1 and c_2 are two fixed, positive parameters called *cognitive* and *social* parameter, respectively; r_1, r_2 are random numbers uniformly distributed in $[0,1]$; and q stands for the counter of iterations. The objective function, f , is computed again at the new positions $X_i^{(q+1)}$ of the particles, and the best positions, $P_i, i=1,2,\dots,N$, are updated along with the new indices g_i . Then, Eqs. (5) and (6) are applied again to proceed to the next iteration of the algorithm. The procedure stops when a sufficiently good solution is detected or a maximum number of iterations is reached.

Let us now discuss the role of the various parameters that appear in equations (5) and (6). The constriction factor, χ , is used as a mechanism to control and adjust the magnitude of the velocities. Cognitive parameter c_1 controls the effect of the knowledge of the best previous position, P_i , of i-th particle on its velocity, while social parameter c_2 plays a similar role but it concerns the best previous position, P_{g_i} , attained by any particle in the neighborhood. The size, N , of the swarm as well as the neighborhood radius, r , are usually set arbitrarily. However, it is a common belief in evolutionary computation that a population size equal from 2 to 10 times the dimension of the problem at hand is a good initial guess. Moreover, the neighborhood's size shall be problem-dependent. In easy problems, larger neighborhoods result in faster convergence without loss of the algorithm's efficiency, while, in harder problems with a plethora of local minima, smaller neighborhoods are considered a better starting choice.

1.2 Detecting further minimizers thought Deflection

PSO is able to detect one, in general arbitrary, minimizer of the objective function, per run. However, in some applications, several minimizers of the objective function are required. Restarting the algorithm does not guarantee the detection of a different minimizer. In such cases, the *deflection* technique can be used. This technique consists of a transformation of the objective function, f , once a minimizer X_i^* , $i=1,\dots,n_{\min}$, has been detected^[2],

$$F(X) = [\tanh(\lambda_i \|X - X_i^*\|)]^{-1} f(X), \quad (7)$$

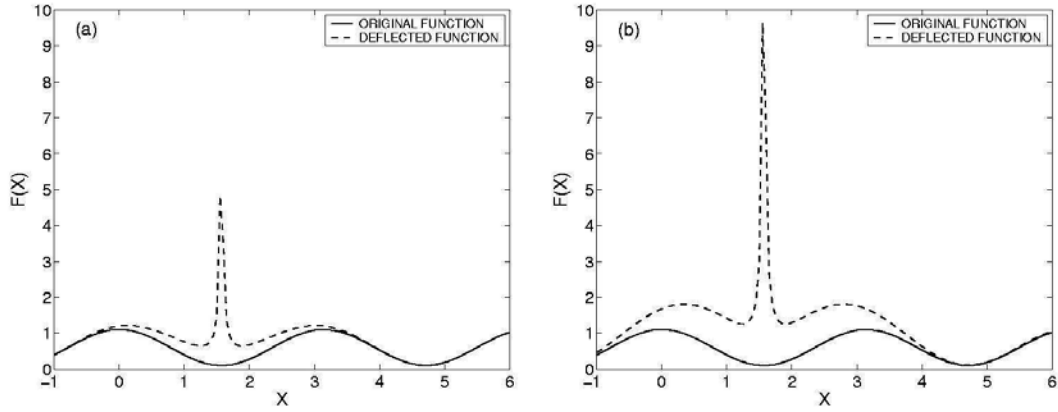


Figure 1. The effect of the deflection procedure on the function $f(x) = \cos^2x + 0.1$, at the point $x^* = \pi/2$, for $\lambda=1$ (a), and $\lambda=0.5$ (b).

where λ_i , $i = 1, \dots, n_{\min}$, are nonnegative relaxation parameters, and n_{\min} is the number of the detected minimizers. The transformed function, F , has exactly the same minimizers with f , with the exception of X_i^* . Alternative configurations of the parameter λ result in different shapes of the transformed function. For larger values of λ , the impact of the deflection technique on the objective function is relatively mild. On the other hand, using $0 < \lambda < 1$, results in a function, F , with considerably larger function values in the neighborhood of the deflected minimizer.

A point to notice is that the deflection technique should not be used on its own on a function f , whose global minimum is zero. The reason is that the transformed function F , of Eq. (7), will also have zero value at the deflected global minimizer, since f will be equal to zero at such points. This problem can be easily alleviated by taking $f = f + c$, where $c > 0$ is a constant, instead of f . The function f possesses all the information regarding the minimizers of f , but its global minimum is increased from zero to c . The value of c does not affect the performance of the algorithm and, thus, if there is no information regarding the global minimum of f , it can be selected arbitrarily large. The effect of the deflection procedure on the function $f(x) = \cos^2x + 0.1$, at the point $x^* = \pi/2$, is illustrated in Fig. 1.

2 THE GALACTIC POTENTIAL

The 3D galactic bar model that is used in our study is described in detail by Skokos et al.^[3]. It consists of a Miyamoto disk, a Plummer bulge and a Ferrers bar. The potential of the Miyamoto disk^[4] is given by the formula,

$$V_D = - \frac{G M_D}{\sqrt{x^2 + y^2 + \left(A + \sqrt{B^2 + z^2}\right)^2}}, \quad (8)$$

where M_D represents the total mass of the disk, A and B are the horizontal and vertical scale lengths, respectively, and G is the gravitational constant. The bulge is a Plummer sphere, i.e., its potential is given by

$$V_S = - \frac{G M_S}{\sqrt{x^2 + y^2 + z^2 + \varepsilon_s^2}}, \quad (9)$$

where ε_s is the bulge scale length and M_S is its total mass. Finally, the bar is a triaxial Ferrers bar with density defined by

$$\rho(m) = \begin{cases} \frac{105 M_B}{32 \pi abc} (1-m^2)^2 & \text{for } m \leq 1 \\ 0 & \text{for } m \geq 1 \end{cases} \quad (10)$$

where

$$m^2 = \frac{y^2}{a^2} + \frac{x^2}{b^2} + \frac{z^2}{c^2}, \quad a > b > c, \quad (11)$$

a , b , c are the principal semi-axes, and M_B is the mass of the bar component. The corresponding potential is denoted by V_B .

For the Miyamoto disk we use $A=3$ and $B=1$, and for the axes of the Ferrers bar we set $a:b:c = 6:1.5:0.6$. The masses of the three components satisfy $G(M_D+M_S+M_B)=1$. In particular we have $GM_D=0.82$, $GM_S=0.08$, $GM_B=0.10$ and $\varepsilon_s=0.4$. The length unit is taken as 1 kpc, the time unit as 1 Myr and the mass unit as 2×10^{11} solar masses. The bar rotates with a pattern speed $\Omega_b=0.054$ around the z -axis, which corresponds to 54 km/(sec kpc) and places corotation at 6.13 kpc. For the scaling of units used see [3].

The Hamiltonian governing the motion of a test particle can be written in the form

$$H = \frac{1}{2} (p_x^2 + p_y^2 + p_z^2) + V_D + V_S + V_B - \Omega_b (x p_y - y p_x) \quad (12)$$

with p_x , p_y , p_z being the canonical momenta. The numerical value of H is also reported as the 'energy' of the system.

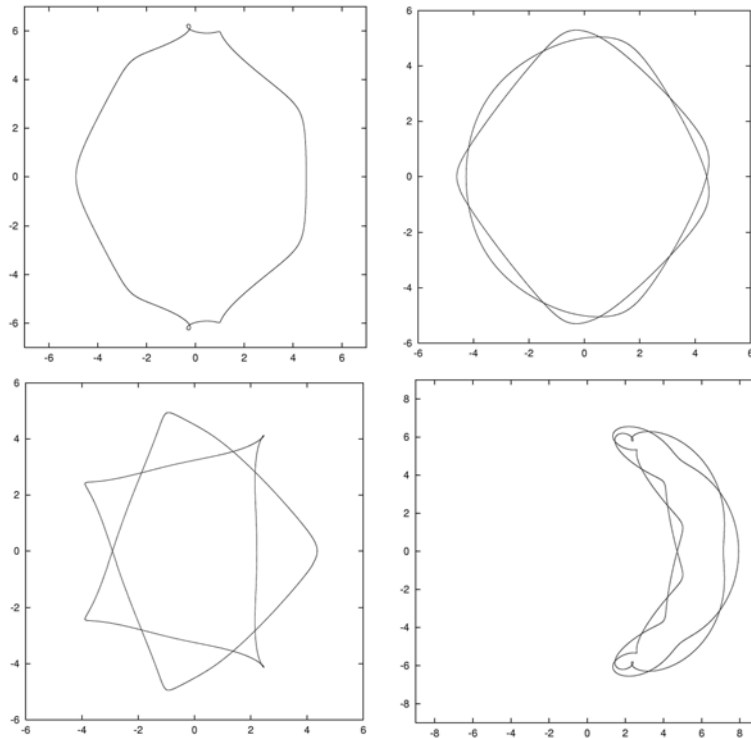


Figure 2. 2D stable orbits plotted on the xy plane. The 1-periodic orbit of the upper left panel is influenced by the 9:1 resonance. All other orbits are of period 2.

3 TRACING PERIODIC ORBITS

The Poincaré Surface of Section (PSS) of the Hamiltonian system defined by Eq. (12) is a 4-dimensional space defined by the conditions $y=0, \dot{y}>0$. Solving numerically the Hamilton's equations of motion results in the time evolution of orbits in this system. Therefore, for a given value of the energy, H , an orbit with initial conditions $X_0=(x_0, z_0, \dot{x}_0, \dot{z}_0)^T$ on the PSS, is propagated in time and its next intersection with the PSS is denoted as

$$\Phi(X_0)=(\Phi_x(X_0), \Phi_z(X_0), \Phi_{\dot{x}}(X_0), \Phi_{\dot{z}}(X_0))^T : \mathbb{R}^4 \rightarrow \mathbb{R}^4. \quad (13)$$

By using the notation $\Theta_4=(0,0,0,0)^T$, the initial conditions X of a p -periodic orbit of the system satisfy the equations

$$\Phi^p(X) = X \Rightarrow \Phi^p(X) - X = \Theta_4 \Rightarrow \begin{pmatrix} \Phi_x^p(X) \\ \Phi_z^p(X) \\ \Phi_{\dot{x}}^p(X) \\ \Phi_{\dot{z}}^p(X) \end{pmatrix} - \begin{pmatrix} x \\ z \\ \dot{x} \\ \dot{z} \end{pmatrix} = \begin{pmatrix} 0 \\ 0 \\ 0 \\ 0 \end{pmatrix}. \quad (14)$$

Thus, finding the initial conditions, X , of a p -periodic orbit is equivalent to solving Eq. (14), which in turn is equivalent to computing the global minimizers of the objective function

$$f(X) = (\Phi_x^p(X) - x)^2 + (\Phi_z^p(X) - z)^2 + (\Phi_{\dot{x}}^p(X) - \dot{x})^2 + (\Phi_{\dot{z}}^p(X) - \dot{z})^2. \quad (15)$$

This technique transforms the problem of finding periodic orbits to the corresponding global minimization problem. The objective function, f , is minimized for different values of the energy through the local version of PSO. The deflection technique is also incorporated in order to find several periodic orbits of a certain period, p . We used the default values of the parameters of PSO, i.e., $\chi=0.729, c_1=c_2=2.05$, which have proved to be optimal with respect to the stability analysis of the model defined by Eqs. (5) and (6)^[1]. The swarm size was $N=20$, and the neighborhood size for each particle was equal to 3. Regarding deflection, the parameters $\lambda=10^4, c=0.1$, were used^[5].

Using the above scheme we were able to find, apart from the known 1-periodic orbits of the system^[3], many new 2D and 3D orbits of period 1, as well as orbits of period 2 and 3. A sample of these new orbits is presented in Figs. 2 (2D orbits) and 3 (3D orbits). We note that all orbits of Figs. 2 and 3 are stable. A detailed registration of the newly computed orbits, as well as a study of their importance for the dynamics of the bar, are currently under consideration and will be reported in the near future.

4 ACKNOWLEDGEMENTS

Ch. Skokos was supported by the Research Committee of the Academy of Athens, the 'Karatheodory' post-doctoral fellowship No 2794 of the University of Patras and the Greek Scholarships Foundation. This work was also partially supported by the 'Pythagoras' research grant awarded by the Greek Ministry of Education and Religious Affairs and the European Union.

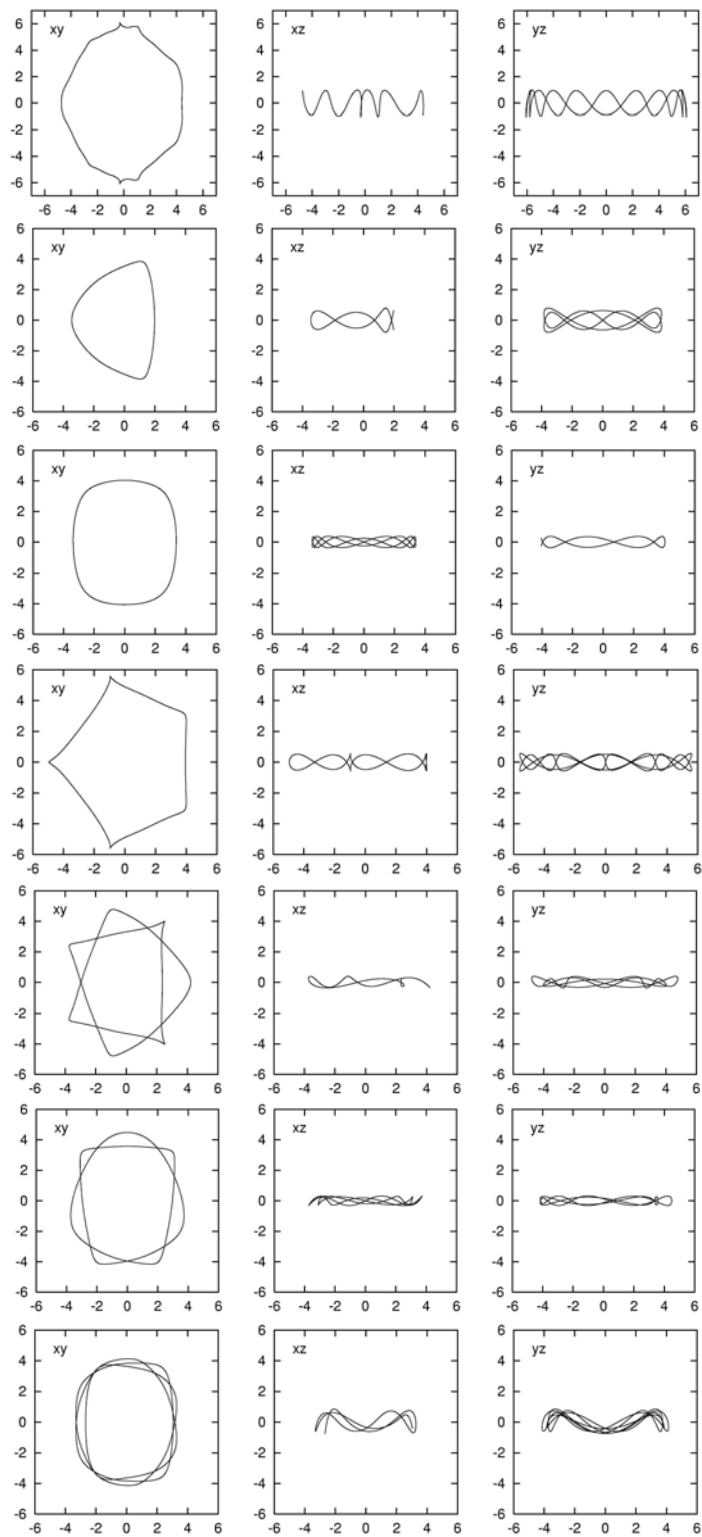


Figure 3. 3D stable orbits. The orbit of the first row is 1-periodic, while the orbit of the last row is 3-periodic. All others orbits are of period 2. The projection planes are indicated in the upper left corner of each frame.

REFERENCES

- [1] Clerc M. and Kennedy J. (2002), “The Particle Swarm – explosion, stability, and convergence in a multidimensional complex space”, *IEEE Trans. Evol. Comput.*, 6(1), 58.
- [2] Magoulas G. D., Plagianakos V. P. and Vrahatis M. N. (1997), “On the alleviation of the problem of local minima in backpropagation”, *Nonlinear Analysis Theory Methods & Applications*, 30(7), 4545.
- [3] Skokos Ch., Patsis P. A. and Athanassoula E. (2002), “Orbital dynamics of three-dimensional bars – I. The backbone of three-dimensional bars. A fiducial case”, *Monthly Notices of the Royal Astronomical Society*, 333, 847.
- [4] Miyamoto M and Nagai R. (1975), “Three-dimensional models for the distribution of mass in galaxies”, *Publications of the Astronomical Society of Japan*, 27, 533.
- [5] Parsopoulos, K.E., Vrahatis, M.N. (2004), “On the Computation of All Global Minimizers Through Particle Swarm Optimization”, *IEEE Transactions on Evolutionary Computation*, 8 (3), 211.